Dissociative Carbamate Exchange Anneals 3D Printed Acrylates

Leslie S. Hamachi,[†, ‡] Daniel A. Rau,[§] Clay B. Arrington,[⊥] Daylan T. Sheppard,[†]
David J. Fortman,[†, ∥] Timothy E. Long,[#] Christopher B. Williams,[§] and William R. Dichtel[†,*]

[†]*Department of Chemistry, Northwestern University, 2145 Sheridan Road, Evanston, IL, 60208 USA*

[‡]*Department of Chemistry and Biochemistry, California Polytechnic State University, San Luis Obispo, California, 93407 USA*

[§]*Department of Mechanical Engineering, Macromolecules Innovation Institute, Virginia Tech, Blacksburg, VA, 24061, USA*

[⊥]*Department of Chemistry, Macromolecules Innovation Institute, Virginia Tech, Blacksburg, VA, 24061, USA*

[∥]*Department of Chemistry and Chemical Biology, Cornell University, Baker Laboratory, Ithaca, New York, 14853 USA*

[#]*School of Molecular Sciences, Biodesign Center for Sustainable Macromolecular Materials and Manufacturing, Arizona State University, Tempe, AZ, 85281, USA*

Keywords: covalent adaptable network, dissociative carbamate exchange, vat photopolymerization, additive manufacturing, polyurethane, 3D printing

Abstract

Relative to other additive manufacturing (AM) modalities, vat photopolymerization (VP) offers designers superior surface finish, feature resolution, and throughput. However, poor interlayer network formation can limit a VP-printed part's tensile strength along the build axis. We demonstrate that incorporation of carbamate bonds capable of undergoing dissociative exchange reactions provides improved interlayer network formation in VP-printed urethane acrylate polymers. In the presence of dibutyltin dilaurate (DBTDL) catalyst, exchange of these carbamate bonds enables rapid stress relaxation with an activation energy of 133 kJ/mol, consistent with a dissociative bond exchange process. Annealed XY tensile samples containing catalyst demonstrate a 25% decrease in Young's modulus attributed to statistical changes in network topology, while samples without catalyst show no observable effect. Annealed ZX tensile samples printed with layers perpendicular to tensile load demonstrate an increase in elongation at break indicative of self-healing. The strain at break for samples containing catalyst increase from 33.9% to 56.0% after annealing but decreases from 48.1% to 32.1% after annealing in samples without catalyst. This thermally activated bond exchange process improves the performance of VP-printed materials via self-healing across layers and provides a means to change the Young's modulus after printing. Thus, the incorporation of carbamate bonds and appropriate catalysts in the VP-printing process provides a robust platform for enhancing material properties and performance.

Introduction

Incorporation of dynamic covalent bonds into additively manufactured polymers has recently been employed to address weak layer interfaces perpendicular to the loading direction.[1] Historically, this mode of material failure has been addressed by processing innovations like infrared pre-heating,[2] z-pinning,[3] and multi-axis printing,[4] or by chemistry innovations like incorporating increased van der Waals[5] or supramolecular interactions.[6-9] More recently, dynamic covalent processes such as Diels-Alder reactions,[10-12] transesterification,[13,14] disulfide exchange[15] or boronate ester exchange[16] triggered after printing have conferred improved interlayer strength. Initial reports focused on the AM of dynamic thermoplastics via fused filament fabrication (FFF),[10,11] with more recent reports focusing on AM of thermosets via direct ink writing,[13] and vat photopolymerization (VP), also referred to as stereolithography (SLA).[14-16]

Although a variety of AM techniques are used to produce tailored polyurethane materials for biomedical applications,[17] most dynamic systems require incorporation of ester, disulfide, or Diels-Alder linkages. Many of these covalent adaptable network (CAN) linkages are more labile than carbamate bonds, which could cause creep under certain conditions, analogous to polymers linked via weakly associated supramolecular interactions.[1] Fortunately, recent efforts have studied the mechanism of associative and dissociative carbamate exchange in cross-linked polyurethane networks, demonstrating the carbamate bond itself to be dynamic at elevated temperatures.[18] Indeed, this exchange process was recently employed to improve the properties of materials in polymer powder bed fusion AM processes.[19] Here we extend the utility of carbamate exchange mediated self-healing to VP-printed materials. This process will enable interfacial layer healing in VP-printed thermoset polyurethanes, broadening the use of commercial urethane acrylate materials

in this process without requiring the design of new resins that incorporate more labile dynamic bonds.

Although dynamic covalent chemistry has been demonstrated to perform self-healing of materials and allow VP-printed materials to be recycled,[13-15] the effect of thermally annealing VP-printed CANs post-print has not rigorously been explored. Previous reports of VP-printed polyester CANs showed a stiffening of materials following a thermal cure; however, these were not compared with catalyst-free control samples.[14] Annealing has previously been applied in the context of polymers to help drive polymerization reactions to completion, and remove solvent;[20] however, the effect of thermally activated bond exchange processes on topological defects in polymers has only recently been studied. In non-dynamic polymer hydrogel systems, eliminating polymer loops increased the shear elastic moduli (G') by up to 600%.[21,22] More recently, eliminating loop defects in acrylic diblock copolymer CANs via vinylogous urethane exchange provided an increase in elastically effective cross-links.[23] Further theoretical work predicts that polymers containing loop defects relax stress faster than networks in which loops cannot form.[24]

We hypothesized dynamic covalent bonds would similarly alter the mechanical properties of VP-printed CANs upon annealing via changes in polymer topology due to the dynamic nature of the carbamate cross-links. Here, we study both the self-healing at layer interfaces and changes in Young's moduli of thin-film and VP-printed urethane acrylates that undergo dissociative carbamate exchange in the presence of a tin catalyst. The tin-catalyzed mechanism allows a direct comparison of films printed with and without catalyst to differentiate the effects of thermal conversion and thermal stress relaxation on VP-printed material properties. The relative magnitude of these two competing effects changes as a consequence of initial UV exposure intensity during the VP-printing process. Upon annealing, we observe evidence of self-healing via SEM of fracture

surfaces and an increased strain at break in ZX tensile samples (21.1% increase) compared to a decrease in control samples without catalyst (16.0% decrease). Additionally, we find that the Young's modulus decreases for samples containing catalyst, whereas the modulus of control samples without catalyst are unchanged. This has many important implications, one being that the stiffness of VP-printed materials can be tuned via incorporation of dynamic covalent bonds while maintaining their structural integrity.

Results and Discussion

Cross-linker Synthesis.

An acrylate crosslinker containing carbamate bonds (**1**) was synthesized via the reaction of toluene diisocyanate with 2-hydroxyethyl acrylate in the presence of a dibutyltin dilaurate (DBTDL) catalyst (Scheme S1). The crosslinker **1**, could be isolated in 98% yield as a fine white powder with (<1 ppm) residual tin as determined by elemental analysis (ICP-OES) following an optimized workup procedure. To prevent unwanted photopolymerization, **1** was stored in a -18 °C freezer in the absence of light.

Thin-Film Polymer Synthesis.

To prepare a photopolymerizable resin **IN-15**, 8.16 g of crosslinker (**1**) was dissolved in 32.6 mL of butyl acrylate which produces a resin where 15% of the acrylates come from the crosslinker. This sample was directly compared with **IC-15** which is prepared with the addition of DBTDL that enables thermally-activated carbamate exchange. Samples labeled with an **IC-** or **IN-** contain crosslinker that was isolated and purified before use. As an alternative method, the crosslinker could also be prepared *in-situ* with butyl acrylate as the reaction solvent. This eliminates the need

for a crosslinker purification step as long as the final resin contains DBTDL. Additional monomer and DBTDL were added at various mole ratios to prepare resins **C-5**, **C-10**, **C-15**, and **C-20** (See SI). Samples labeled with a **C-** contain crosslinker synthesized *in-situ* before diluting with butyl acrylate and adding DBTDL. We observed nearly identical properties from samples **C-15** and **IC-15** which are synthesized via two different methods but result in the same final resin composition. Prior to photopolymerization, diphenyl(2,4,6-trimethylbenzoyl)phosphine oxide (TPO) photoinitiator was added at 2 wt. % to all resins and sonicated to dissolve. To generate thin-film specimens, the resin was photopolymerized under a Bevili Color 80W UV LED Nail Curing Chamber in between glass slides to minimize radical inhibition via oxygen (Figure 1).

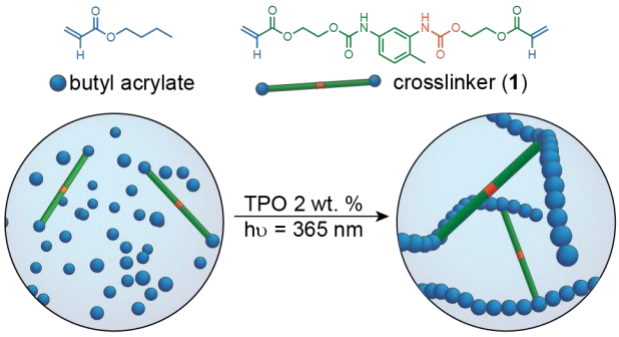

Figure 1. Butyl acrylate and (**1**) are photopolymerized with 2 wt. % TPO to form urethane acrylate cross-linked networks.

Photopolymerization kinetics were monitored via Fourier transform infrared spectroscopy (FTIR, Figure 2A). Resins were cured for 0-60 seconds followed by analysis via FTIR (Figure S3). Following literature precedent, the acrylate C=C double bond absorption intensity at 810 cm^{-1} was measured relative to the unchanging C=O absorption intensity at 1727 cm^{-1} to calculate acrylate double bond conversion.[25,26] The conversion of acrylate C=C double bonds appears complete, relative to the detection limit of the spectrometer, after 20 seconds. Nevertheless, in order to ensure full photopolymerization, a cure time of 60 seconds was used for model thin-films (Figure S4). Differential Scanning Calorimetry (DSC) was also used to assess the completeness of

film curing. The T_g of films **IC-15** and **IN-15** cured for 60 seconds were compared with films cured for 10 minutes on each side. We find that the T_g does not significantly increase between curing conditions, corroborating the FTIR results that 60 seconds is a sufficient curing time for model thin-films photopolymerized in the nail curing chamber (Figure S5).

Photorheology measurements to characterize the curing kinetics of **C-5** and **C-15** resins show rapid curing and a high cured storage modulus (Figure 2B). Both resins exhibited cross-over times below 3 seconds, which is sufficiently fast for use in VP printing. As expected, the **C-15** resin had a higher cured modulus than the **C-5** resin due to the additional crosslinker incorporation.

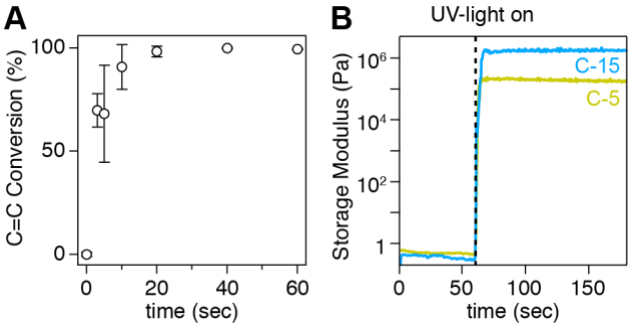

Figure 2. Urethane acrylate curing kinetics were observed via (A) FTIR and (B) photorheology. Photorheology measurements of the **C-5** and **C-15** resin showed extremely rapid gelation. UV irradiation began at 60s.

By varying the crosslinker concentration (samples **C-5**, **C-10**, **C-15**, and **C-20**), the tensile strength of the resulting photopolymer was tuned from 0.277 to 3.34 MPa (Figure S6, Table S3). As the percent incorporation of the crosslinker increases, the calculated M_w between crosslinkers (see SI for details) varies from 1630 g/mol to 369 g/mol. This change is accompanied by a change in T_g from -38 °C to 5 °C, as determined by DSC and DMTA (Figure S7-10, Table S4). Gel fractions of the photopolymerized samples were determined by swelling in CH_2Cl_2 for 48 hours followed by drying the polymers at room temperature under 20 mtorr vacuum for 48 hours. Swell tests of the photopolymerized samples show over 97% gel fraction of the material (Table S4). Notably, all urethane acrylate thin-films containing DBTDL catalyst relax stress at elevated

temperatures (Figure S11, Table S5). Subsequent experiments use the **IC-15** and **IN-15** resins, which provide desirable tensile properties without approaching the solubility limit of crosslinker in resin at room temperature.

We hypothesized that annealing the urethane acrylate photopolymers would result in the increased formation of covalent bonds across the layers of a VP-printed structure due to a thermally activated carbamate exchange process (Figure 3A). Based on prior studies, the most likely mechanism for carbamate exchange is the transient reversion of carbamate groups to isocyanates and alcohols, which reform into new carbamate linkages. Notably, the tin catalysts employed in dissociative carbamate exchange processes are deactivated in the presence of excess free alcohol.[18] Therefore, this limits the scope of monomers that can be used to ones that do not contain alcohols and informed the choice of butyl acrylate as the monomer in this study. The carbamate bond exchange process is commonly characterized via stress relaxation analysis (SRA). Thus, to develop appropriate annealing conditions, SRA was used to characterize the rate of topological reorganization in **IC-15** thin-films at different temperatures (Figure 3B, Figure S6). The characteristic relaxation times (τ^*) are plotted vs. 1000/T to determine an activation energy of 133 kJ/mol for the dissociative carbamate exchange process (Figure 3C). This activation energy is consistent with activation energies reported for dissociative carbamate exchange in polyether polyurethane (143 kJ/mol) and polyester polyurethane (144 kJ/mol) systems,[27] and higher than activation energies observed in the alcohol-mediated associative transcarbamoylation exchange in polyhydroxyurethanes (111 kJ/mol).[28] Based on the absence of free alcohols and the experimentally determined activation energy, the exchange mechanism is thought to be dissociative. **IN-15** thin-films prepared without the DBTDL catalyst do not relax stress

significantly in similar timeframes, corroborating previous findings that the DBTDL catalyst is required for rapid carbamate reversion reactions.

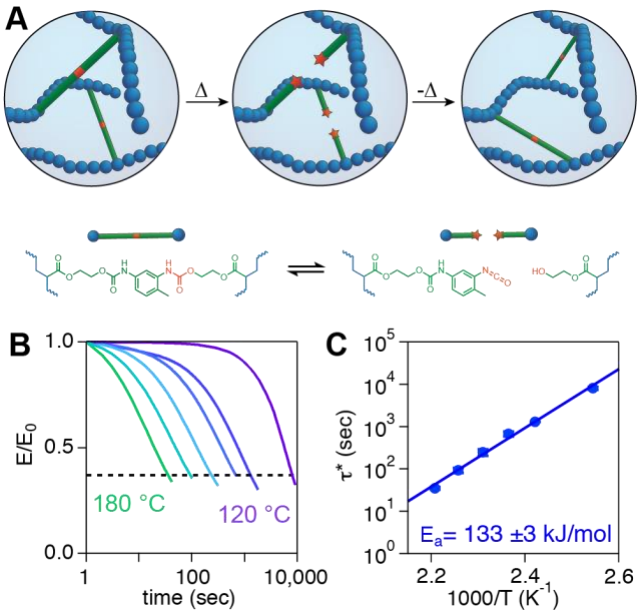

Figure 3. (A) Dissociative carbamate exchange mechanism of stress relaxation, (B) stress relaxation curves of **IC-15** at different temperatures, (C) Arrhenius plot to determine activation energy.

Based on the temperature dependent stress relaxation results, two annealing conditions were selected: 1 hour at 160 °C and 24 hours at 120 °C. Both of these annealing conditions are over ten times τ* at the given temperature, thus allowing for significant bond exchange to occur. Although stress relaxation is most rapid at elevated temperatures, the thin-films begin to discolor at extended annealing times (Figure S12-13). We attempted to chemically characterize this discoloration process by comparing FTIR spectra of thin-films pre- and post-anneal. However, no discernible changes could be observed (Figure S14). Thermogravimetric analysis (TGA) shows that films begin to irreversibly decompose at temperatures above 240 °C; however, holding at a temperature of 160 °C results in negligible mass loss (Figure S15-18). Thus, annealing at 160 °C for 1 hour hastens stress relaxation in the catalyst-containing **IC-15** samples while avoiding film

degradation and minimizing discoloration. Control samples of **IN-15** were subject to the same annealing conditions to isolate the effect of thermal annealing on carbamate exchange.

Mechanical Properties After Annealing

We observe that annealing the model thin-film samples containing catalyst results in a decrease in the Young's modulus and stiffness of the polymers, whereas annealing samples without catalyst results in no change (Figure 4, Table 1, Figure S19-20). The Young's modulus of **IC-15** thin-films decreases from 3.09 ± 0.08 MPa to 2.33 ± 0.07 MPa when annealed at 120 °C for 24 hours, whereas the Young's modulus of **IN-15** thin-films stays constant (3.19 ± 0.08 MPa to 3.15 ± 0.11 MPa) under similar annealing conditions. One plausible explanation is that the DBTDL causes carbamate reversion reactions without re-forming new carbamate bonds, which would decrease network cross-linking and lead to higher strain at break. However, DMTA data obtained before and after annealing appear identical (Figure 4C), indicating that this is unlikely. Thus, we hypothesize that either a removal of internal stresses or rearrangement of the polymer topology via introduction of loop defects is responsible for this decrease in Young's modulus while maintaining network connectivity. Indeed, theoretical studies have speculated that the modulus of CANs could be switched by annealing under conditions favoring different loop statistics, in contrast with thermoset elastomers possessing a fixed loop content.[24]

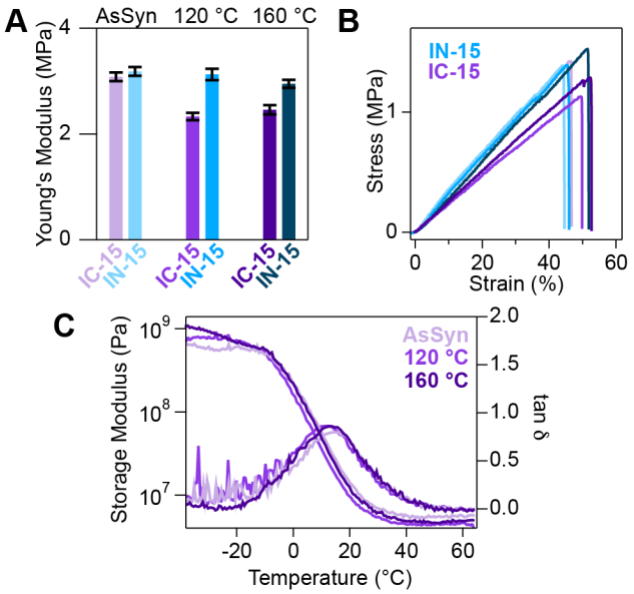

Figure 4. (A) Comparison of Young's moduli for polymer thin-films of **IC-15** with catalyst (shades of purple) and **IN-15** without catalyst (shades of blue) at different annealing conditions. Annealing at 120 °C was performed for 24 hours, and annealing at 160 °C was performed for 1 hour. (B) Representative tensile testing data of polymer thin-films of **IC-15** and **IN-15** at different annealing conditions noted in A. (C) DMTA of polymer thin-films of **IC-15** pre- and post-annealing.

Table 1. Tensile properties of the polymer thin-film networks pre- and post-anneal.

Polymer	σ_b (MPa) As-Synthesized	σ_b (MPa) Annealed 120 °C, 24 hr	σ_b (MPa) Annealed 160 °C, 1 hr	ε_b (%) As-Synthesized	ε_b (%) Annealed 120 °C, 24 hr	ε_b (%) Annealed 160 °C, 1 hr	*E* (MPa) As-Synthesized	*E* (MPa) Annealed 120 °C, 24 hr	*E* (MPa) Annealed 160 °C, 1 hr
IC-15 Thin-films	1.469 ± 0.109	1.140 ± 0.068	1.283 ± 0.088	47.58 ± 3.04	48.82 ± 3.02	52.13 ± 2.31	3.09 ± 0.08	2.33 ± 0.07	2.46 ± 0.09
IN-15 Thin-films	1.383 ± 0.137	1.460 ± 0.134	1.433 ± 0.224	43.36 ± 3.60	46.29 ± 4.15	48.44 ± 6.96	3.19 ± 0.08	3.15 ± 0.11	2.95 ± 0.07

VP Printing

Tensile bars were printed using top-down Mask-Projection (MP) VP, also referred to as Stereolithography (SLA) or Digital Light Processing (DLP), to assess the improved interlayer network formation hypothesis and to evaluate the effect of stress relaxation on VP-printed parts. Compared to model thin-films cured at a set thickness and UV flux, the mechanical properties of VP-printed materials are dependent on printing parameters, including the amount of UV exposure

each layer receives, the layer thickness, and any UV post-curing. These observations are consistent with literature reports of (meth)acrylate resins printed with variable UV exposure conditions producing different network crosslinked densities, where higher exposures produce parts with a higher modulus and T_g.[29] This effect has also been observed in polyurethane acrylates with a threefold increase in elastic modulus based on a fourfold increase in light intensity.[30] Recent work on a VP-printed thiol-ene resin further explores the relationship between light intensity at a constant dose and local conversion using nanocylinder-tipped atomic force microscopy and a rheo-Raman microscope.[31]

For analysis of the VP-printed material under various print conditions without the confounding effect of layer interfaces, XY tensile bars were printed with loading parallel to the layer interfaces based on the ISO/ASTM 52921 standard.[32] To accurately explore the mechanical properties of VP-printed XY tensile bars from resins **IC-15** and **IN-15**, UV exposure times for each layer of 6 sec (low) and 20 sec (high) were used with an intensity of 14 mW/cm^2 at 405 nm, as measured by an ILT800-UVF radiometer. The low exposure time was the minimum necessary for adequate interlayer curing and part strength, while the high exposure time was the maximum exposure before overcuring occurred, sacrificing feature resolution. Congruent with literature precedent, over this range of UV exposures, the material properties were tuned from a "soft" to "hard" sample exhibiting higher modulus, ultimate tensile strength (UTS), and T_g as measured by tensile testing and DMA (Figure 5). Despite the slight increase in elastic modulus observed in the high exposure printed sample relative to the model film samples, the VP-printed XY sample of **IC-15** demonstrates rapid stress relaxation at 160 °C comparable to the model films (153sec vs. 359 sec). The variations in exposure time per layer resulted in minimal discernable difference in stress relaxation behavior (Low Exposure: 199 sec, High Exposure: 153 sec, High Exposure +

Postcure: 320 sec). Thus, the annealing conditions optimized for the model film system could be applied to the VP-printed samples regardless of exposure time.

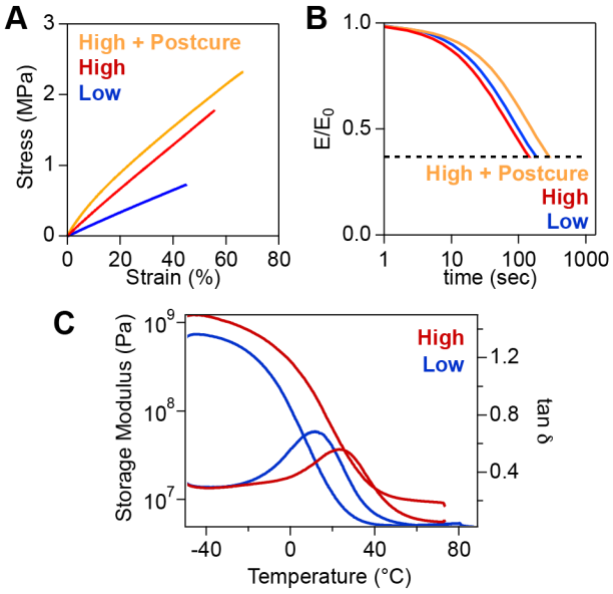

Figure 5: (A) Tensile testing of VP-printed XY tensile bars (resin **IC-15**) at Low exposure (6 s per layer), High exposure (20 s per layer), and High + Postcure (20 s per layer, followed by 20 min in a UV chamber post-printing). (B) Stress relaxation data of VP-printed rectangular bars at 160 °C, prepared under the same conditions as A. (C) DMA of VP-printed objects at low exposure and high exposure.

Analogous to the effect observed in model thin-films, pre- and post-anneal testing of XY tensile bars printed from resin **IC-15** (containing carbamate exchange catalyst) generally demonstrate a decrease in Young's modulus whereas samples printed from resin **IN-15** (catalyst free) show an increase (Figure 6, Figure S21-22, Table S7). For resins **IC-15** and **IN-15**, both "low" and "high" exposure samples were printed, annealed (Figure S23), and tested to observe the effect of annealing on these two as-printed extremes. Upon annealing **IC-15** XY tensile bars, the "low" and "high" exposure samples annealed at 160 °C for 1 hour both exhibit a decrease in Young's modulus. When annealed at 120 °C for 24 hours, the "low" and "high" exposure **IC-15** XY tensile bars do not exhibit a significant decrease in Young's modulus. After annealing, the

catalyst-containing "low" exposure samples demonstrated an increase in both stress and strain, whereas the "high" exposure samples demonstrated a decrease in stress and increase in strain at break. For both sets of samples, annealing for 1 hour at 160 °C had a more pronounced effect than annealing for 24 hours at 120 °C. Notably for these VP-printed XY samples, the stress relaxation time was only characterized at 160 °C (Figure 5). Thus, observed differences based on annealing condition might be due to incomplete stress relaxation at 120 °C based on slight differences between the VP-printed samples and model thin-films. In contrast with these observed decreases in Young's modulus for VP-printed **IC-15** samples, the post-anneal behavior of the "low" and "high" exposure VP-printed **IN-15** XY tensile bars demonstrated a slight increase in modulus after annealing (Table S7).

Two effects are likely the cause of these observed changes in Young's modulus for the VP-printed XY tensile bars: 1) Stress relaxation decreases the elastic moduli of **IC-15** XY tensile bars via annealing defects while maintaining a set crosslink density, as observed in the model thin-films (Figure 4). 2) A thermal cure increases the elastic moduli, as the increased temperature induces the crosslinking of residual acrylate groups. This effect is more pronounced in the "low" exposure samples as the short initial curing time leaves more unreacted acrylate groups. Supporting this hypothesis, FTIR data of the SLA printed **IN-15** samples initially show a small acrylate C=C peak in the as-printed samples. This peak disappears upon annealing at 160 °C (Figure S24). Furthermore, thermal rheology experiments using a step and hold to 160 °C and 120 °C on **IN-15** resin demonstrate thermal curing with gelation observed in 330 s and 3900 s, respectively, with moduli continuing to increase over an extended period of time at elevated temperatures (Figure S25-27). Of note, we do not observe any unreacted acrylate C=C peaks in the as-printed samples of **IC-15**. These samples only exhibit a decrease in Young's modulus upon annealing. In contrast

with our results, previous studies on photopolymerized dynamic polyester networks, only showed stiffening of materials following a thermal cure.[14] However, these materials were not compared with samples without transesterification catalyst present. Thus, the discrepancy in results may be attributed to different dynamic bond linkages, the different mechanisms of bond dynamicity (associative vs. dissociative), or difficulties distinguishing thermal curing effects from stress relaxation effects, which we study here via inclusion/exclusion of carbamate exchange catalyst.

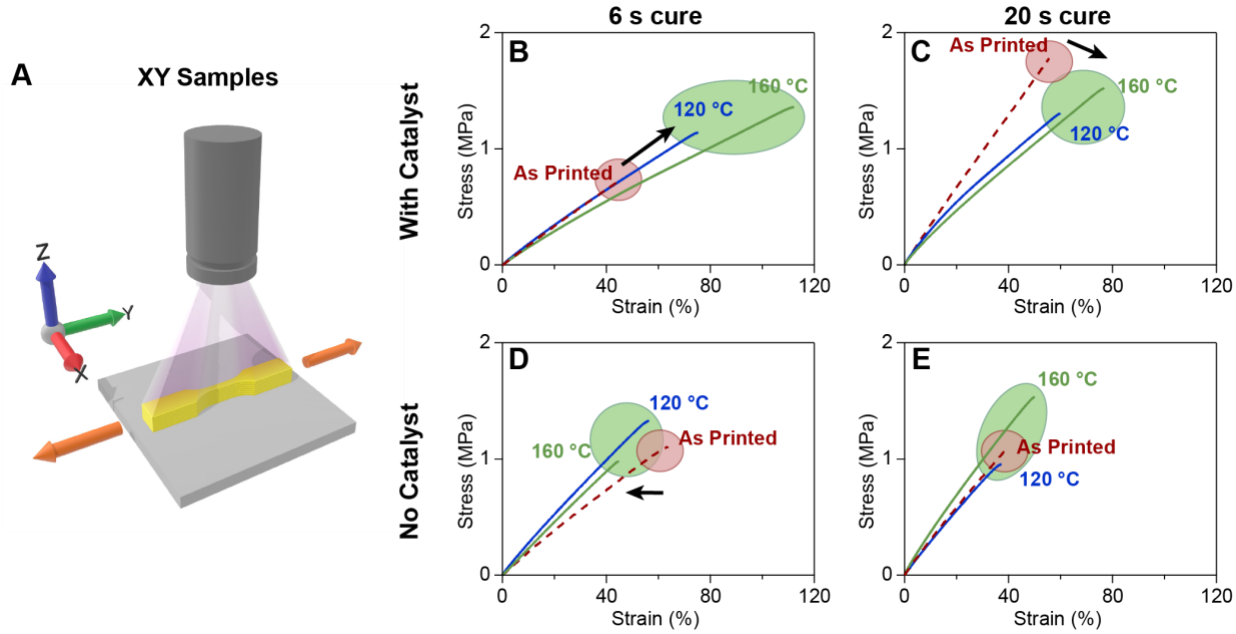

Figure 6: (A) Illustration of XY tensile samples used to evaluate the effect of thermal annealing. Tensile loading was parallel to the layer interfaces. (B-E) Representative tensile testing of VP-printed XY tensile bars before and after thermal annealing at 160 °C for 1 hour or 120 °C for 24 hours. Samples were printed with (B) a 6 second exposure from resin **IC-15**, (C) a 20 second exposure from resin **IC-15**, (D) a 6 second exposure from resin **IN-15**, (E) a 20 second exposure from resin **IN-15**.

To further assess the role of UV exposure on tensile properties before and after annealing, these VP-printed XY tensile sample results were compared with model thin-films photocured for 10 minutes on each side in the nail curing chamber (Figure S28, Table S8). Although the samples cured for 60 seconds were observed to react to similar acrylate C=C bond conversion as films cured for 10 minutes on each side as observable by FTIR, the tensile strength of the as-synthesized

samples increased (**IC-15** increased from 1.469 ± 0.108 MPa to 1.739 ± 0.063 MPa, and **IN-15** increased from 1.383 ± 0.137 MPa to 1.854 ± 0.215 MPa between 60 second and 10 minute cures, respectively) (Figure S28, Table S8). Upon annealing, the model **IC-15** thin-films cured for 10 minutes also exhibit a decrease in Young's modulus, whereas the **IN-15** films remain unchanged (Figure S29). This result is in good agreement with VP-printed XY samples with additional UV postcuring (see Supporting Information), which exhibit an increase in stress at break and decrease in Young's modulus upon annealing (Figure S30).

After probing the effects of the amount of UV exposure, carbamate exchange, and thermal curing on the bulk-like XY samples, the effect of carbamate exchange on interlayer strength was investigated. ZX samples were printed (see Supporting Information) with layers perpendicular to the loading direction based on the ISO/ASTM 52921 standard (Figure 7A).[32] Only high exposure samples with additional UV postcuring were studied because these exposures produced the greatest strength in the as-printed XY tests. Additionally, low exposure samples periodically cracked during the annealing process whereas the high exposure samples did not. The ZX tensile bars were studied after annealing at 160 °C for 1 hour because the 160 °C annealing conditions showed better results than the 120 °C annealing conditions in the XY sample studies.

The profile of the **IN-15** and **IC-15** ZX sample tensile curves were distinct from the XY tensile samples. It is hypothesized that the layer interfaces dominate the mechanical behavior of the ZX samples leading to different tensile profiles and increased variation in mechanical properties. Upon annealing, the ZX samples of **IC-15** (containing catalyst) showed an increase in the elongation at break (Figure 7B, Figure S31, Table S9) from 33.9 ± 10.6% as-printed to 56.0 ± 7.9% post-anneal ($p>0.05$). Changes in modulus ($p=0.69$) and UTS ($p=0.08$) were not statistically significant. Conversely, the ZX samples of **IN-15** (without catalyst), showed a decrease in the

elongation at break (Figure 7C, Figure S31, Table S9) from 48.1 ± 13.9% as-printed to 32.1 ± 7.85% post-anneal. UTS decreased from 1.63 ± 0.26 MPa as-printed to 0.91 ± 0.28 MPa post-anneal ($p>0.05$). Changes in modulus ($p=0.07$) and elongation at break ($p=0.12$) were not statistically significant. We attribute the increase in strain at break for the catalyst-containing samples (22.1% increase compared to the 16.0% decrease in strain at break for samples without catalyst) to dissociative carbamate exchange forming covalent bonds between the printed layer interfaces, strengthening the material. We do not observe significant changes in Young's modulus in these ZX samples which could be a result of the layer interfaces dominating the observed behavior.

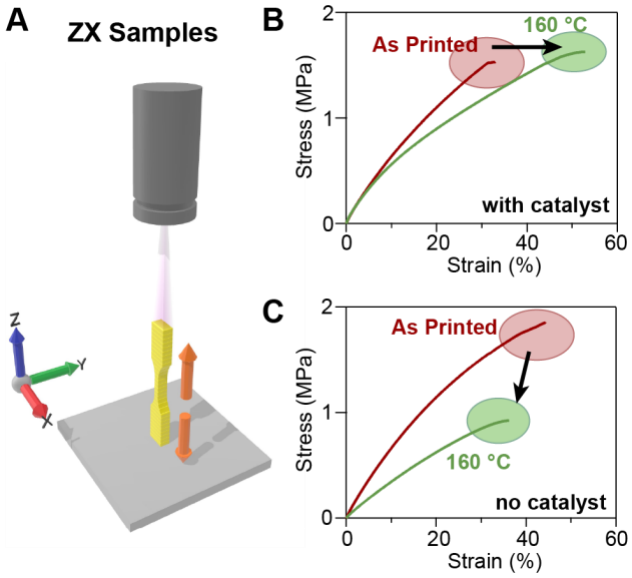

Figure 7: (A) Illustration of ZX tensile samples used to evaluate the effect of thermal annealing. Tensile loading was perpendicular to the layer interfaces. (B) Representative tensile testing of SLA printed (**IC-15**) ZX samples (containing catalyst) before (red) and after (green) thermal annealing. (C) Representative tensile testing of SLA printed (**IN-15**) Z-samples (without catalyst) before (red) and after (green) thermal annealing.

To further probe self-healing in the ZX samples, we characterized the fracture interfaces of the pre- and post-anneal VP-printed tensile samples. Optical microscopy of post-failure ZX

tensile bars shows rough failure surfaces where the effects of annealing cannot be distinguished (Figure S32). In contrast, scanning electron microscopy (SEM) was more illustrative. As-printed samples of **IC-15** are observed to fracture cleanly along layer interfaces (Figure 8A-B), whereas annealed samples of **IC-15** are observed to have rougher fracture surfaces due to improved covalent consolidation between VP-printed layers (Figure 8C-D). This observation is in contrast with clean fracture surfaces observed in annealed samples of **IN-15** (Figure S33). Thus, we conclude from the tensile and microscopy data that carbamate exchange mediated self-healing has occurred between the layer interfaces.

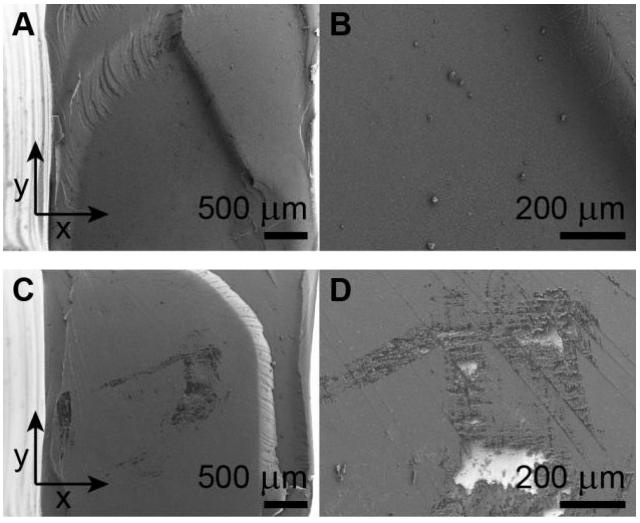

Figure 8. SEM of VP-printed ZX tensile bar fracture surfaces for (A, B) **IC-15** as synthesized, and (C, D) **IC-15** annealed at 160 °C for 1 hour. Right panels (B,D) illustrate surface texture at higher magnification.

In contrast with previous reports on the interfacial welding of polyesters, our observed increase in strain at break of ZX samples occurs in the absence of an external applied pressure. Previous reports find that compression molding is required to increase the amount of bonds that come into contact for exchange.[33] Indeed, whereas disulfide-based CANs can self-heal without an external applied pressure,[34] CANs containing polyester linkages more similar in lability to

carbamates consistently require either pressure or partial dissolution via solvent in order to implement surface welding.[35] We hypothesize that an applied external pressure during annealing could further increase self-healing observed in the ZX samples, although this effect is beyond the scope of this study.

Conclusions

VP-printed urethane acrylate networks undergo stress relaxation and thermal annealing in the presence of a carbamate exchange catalyst such as DBTDL. In VP-printed XY tensile bars and single layer polymer thin-films, the Young's modulus decreases and can be tuned via thermal post-processing. We demonstrate these effects on tensile bars VP-printed under high and low UV exposure. Practical considerations for VP-printing under low UV exposure may result in incomplete photopolymerization that is brought to completion via a thermal cure that increases the modulus. On the other hand, catalyzed urethane exchange processes decrease the material's Young's modulus by up to 25%, possibly via introduction of topological loops or relaxation of internal stresses. Resins prepared without DBTDL catalyst served as a control to explore changes in materials properties that lack dynamic bond exchange. In ZX tensile bars printed such that layers are perpendicular to tensile load and interfacial layer effects dominate, thermal stress relaxation processes improve the ZX tensile strain at break by self-healing between printed layers. The ability of carbamate exchange to self-heal layer interfaces of VP-printed urethane resins and modulate Young's modulus post-print will increase the use of dissociative carbamate exchange in AM processes. Given the ubiquity of urethane acrylates in coatings and as photo-cured resins, these results have potential for broad impact on industrial applications.

ASSOCIATED CONTENT

Supporting Information. The Supporting Information is available free of charge on the ACS Publications website at DOI: [insert DOI]

Monomer synthesis and ^{1}H NMR spectrum, photopolymerization and characterization of urethane acrylate thin-films and VP-printed parts, thermal and mechanical characterization, and additional microscopy. (PDF)

VP-printing video (mp4)

AUTHOR INFORMATION

Corresponding Authors

WRD: wdichtel@northwestern.edu

Notes

The authors declare no conflicts of interest.

Acknowledgement

This work was supported by the NSF Center for Sustainable Polymers, CHE-1901635. DAR and CBW thank Honeywell Federal Manufacturing and Technologies for their generous support. LSH, DAR, CBW, and WRD thank the Honeywell Polymer Additive Manufacturing Consortium administered by Dr. Jamie Messman for introducing the teams and fostering collaboration.

This work made use of the MatCI Facility supported by the MRSEC program of the National Science Foundation (DMR-1720139) at the Materials Research Center of Northwestern University. This work made use of the IMSERC at Northwestern University, which has received support from the Soft and Hybrid Nanotechnology Experimental (SHyNE) Resource (NSF ECCS-1542205), the State of Illinois, and the International Institute for Nanotechnology (IIN).

References

(1) Heidarian, P.; Kouzani, A. Z.; Kaynak, A.; Paulino, M.; Nasri-Nasrabadi, B. Dynamic Hydrogels and Polymers as Inks for Three-Dimensional Printing. *ACS Biomater. Sci. Eng.* **2019**, *5*, 2688-2707.

(2) Kishore, V.; Ajinjeru, C.; Nycz, A.; Post, B.; Lindahl, J.; Kunc, V.; Duty, C. Infrared Preheating to Improve Interlayer Strength of Big Area Additive Manufacturing (BAAM) Components. *Addit. Manuf.* **2017**, *14*, 7-12.

(3) Duty, C.; Failla, J.; Kim, S.; Smith, T.; Lindahl, J.; Kunc, V. Z-Pinning Approach for 3D Printing Mechanically Isotropic Materials. *Addit. Manuf.* **2019**, *27*, 175-184.

(4) Kubalak, J. R.; Wicks, A. L.; Williams, C. B. Using Multi-Axis Material Extrusion to Improve Mechanical Properties Through Surface Reinforcement. *Virtual and Physical Prototyping* **2018**, *13*, 32-38.

(5) Altuna, F. I.; Casado, U.; Dell'Erba, I. E.; Luna, L.; Hoppe, C. E.; Williams, R. J. J. Epoxy Vitrimers Incorporating Physical Crosslinks Produced by Self-Association of Alkyl Chains. *Polym. Chem.* **2020**, *11*, 1337-1347.

(6) Highley, C. B.; Rodell, C. B.; Burdick, J. A. Direct 3D Printing of Shear-Thinning Hydrogels Into Self-Healing Hydrogels. *Adv. Mater.* **2015**, *27*, 5075-5079.

(7) Hart, L. R.; Li, S.; Sturgess, C.; Wildman, R.; Jones, J. R.; Hayes, W. 3D Printing of Biocompatible Supramolecular Polymers and Their Composites. *ACS Appl. Mater. Interfaces* **2016**, *8*, 3115-3122.

(8) Pekkanen, A. M.; Mondschein, R. J.; Williams, C. B.; Long, T. E. 3D Printing Polymers with Supramolecular Functionality for Biological Applications. *Biomacromolecules* **2017**, *18*, 2669-2687.

(9) Chen, X.; Zawaski, C. E.; Spiering, G. A.; Liu, B.; Orsino, C. M.; Moore, R. B.; Williams, C. B.; Long, T. E. Quadruple Hydrogen Bonding Supramolecular Elastomers for Melt Extrusion Additive Manufacturing. *ACS Appl. Mater. Interfaces* **2020**, *12*, 32006-32016.

(10) Davidson, J. R.; Appuhamillage, G. A.; Thompson, C. M.; Voit, W.; Smaldone, R. A. Design Paradigm Utilizing Reversible Diels–Alder Reactions to Enhance the Mechanical Properties of 3D Printed Materials. *ACS Appl. Mater. Interfaces* **2016**, *8*, 16961-16966.

(11) Appuhamillage, G. A.; Reagan, J. C.; Khorsandi, S.; Davidson, J. R.; Voit, W.; Smaldone, R. A. 3D Printed Remendable Polylactic Acid Blends With Uniform Mechanical Strength Enabled by a Dynamic Diels–Alder Reaction. *Polym. Chem.* **2017**, *8*, 2087-2092.

(12) Durand-Silva, A.; Cortés-Guzmán, K. P.; Johnson, R. M.; Perera, S. D.; Diwakara, S. D.; Smaldone, R. A. Balancing Self-Healing and Shape Stability in Dynamic Covalent Photoresins for Stereolithography 3D Printing. *ACS Macro Lett.* **2021**, *10*, 486-491.

(13) Shi, Q.; Yu, K.; Kuang, X.; Mu, X.; Dunn, C. K.; Dunn, M. L.; Wang, T.; Qi, H. J. Recyclable 3D Printing of Vitrimer Epoxy. *Materials Horizons* **2017**, *4*, 598-607.

(14) Zhang, B.; Kowsari, K.; Serjouei, A.; Dunn, M. L.; Ge, Q. Reprocessable Thermosets for Sustainable Three-Dimensional Printing. *Nat. Commun.* **2018**, *9*, 1-7.

(15) Li, X.; Yu, R.; He, Y.; Zhang, Y.; Yang, X.; Zhao, X.; Huang, W. Self-Healing Polyurethane Elastomers Based on a Disulfide Bond by Digital Light Processing 3D Printing. *ACS Macro Lett.* **2019**, *8*, 1511-1516.

(16) Robinson, L. L.; Self, J. L.; Fusi, A. D.; Bates, M. W.; Read de Alaniz, J.; Hawker, C. J.; Bates, C. M.; Sample, C. S. Chemical and Mechanical Tunability of 3D-Printed Dynamic Covalent Networks Based on Boronate Esters. *ACS Macro Lett.* **2021**, *10*, 857-863.
(17) Griffin, M.; Castro, N.; Bas, O.; Saifzadeh, S.; Butler, P.; Hutmacher, D. W. The Current Versatility of Polyurethane Three-Dimensional Printing for Biomedical Applications. *Tissue Eng. Part B Rev.* **2020**, *26*, 272-283.
(18) Brutman, J. P.; Fortman, D. J.; De Hoe, G. X.; Dichtel, W. R.; Hillmyer, M. A. Mechanistic Study of Stress Relaxation in Urethane-Containing Polymer Networks. *J. Phys. Chem. B* **2019**, *123*, 1432-1441.
(19) Sun, S.; Gan, X.; Wang, Z.; Fu, D.; Pu, W.; Xia, H. Dynamic Healable Polyurethane for Selective Laser Sintering. *Addit. Manuf.* **2020**, 101176.
(20) Long, T. E.; Williams, C. B. Printing Nanomaterials in Shrinking Gels. *Science* **2018**, *362*, 1244-1245.
(21) Zhong, M.; Wang, R.; Kawamoto, K.; Olsen, B. D.; Johnson, J. A. Quantifying the Impact of Molecular Defects on Polymer Network Elasticity. *Science* **2016**, *353*, 1264-1268.
(22) Gu, Y.; Kawamoto, K.; Zhong, M.; Chen, M.; Hore, M. J.; Jordan, A. M.; Korley, L. T.; Olsen, B. D.; Johnson, J. A. Semibatch Monomer Addition as a General Method to Tune and Enhance the Mechanics of Polymer Networks via Loop-Defect Control. *Proc. Natl. Acad. Sci. U.S.A.* **2017**, *114*, 4875-4880.
(23) Ishibashi, J. S.; Pierce, I. C.; Chang, A. B.; Zografos, A.; El-Zaatari, B. M.; Fang, Y.; Weigand, S. J.; Bates, F. S.; Kalow, J. A. Mechanical and Structural Consequences of Associative Dynamic Cross-Linking in Acrylic Diblock Copolymers. *Macromolecules* **2021**, *54*, 3972-3986.
(24) Ciarella, S.; Sciortino, F.; Ellenbroek, W. G. Dynamics of Vitrimers: Defects as a Highway to Stress Relaxation. *Phys. Rev. Lett.* **2018**, *121*, 058003.
(25) Lacombe, J.; Soulié-Ziakovic, C. Controlling Self-Patterning of Acrylate Films by Photopolymerization. *Polym. Chem.* **2017**, *8*, 1129-1137.
(26) Ding, R.; Du, Y.; Goncalves, R. B.; Francis, L. F.; Reineke, T. M. Sustainable Near UV-Curable Acrylates Based on Natural Phenolics for Stereolithography 3D Printing. *Polym. Chem.* **2019**, *10*, 1067-1077.
(27) Fortman, D. J.; Sheppard, D. T.; Dichtel, W. R. Reprocessing Cross-Linked Polyurethanes by Catalyzing Carbamate Exchange. *Macromolecules* **2019**, *52*, 6330-6335.
(28) Fortman, D. J.; Brutman, J. P.; Cramer, C. J.; Hillmyer, M. A.; Dichtel, W. R. Mechanically Activated, Catalyst-Free Polyhydroxyurethane Vitrimers. *J. Am. Chem. Soc.* **2015**, *137*, 14019-14022.
(29) Steyrer, B.; Busetti, B.; Harakály, G.; Liska, R.; Stampfl, J. Hot Lithography vs. Room Temperature DLP 3D-Printing of a Dimethacrylate. *Addit. Manuf.* **2018**, *21*, 209-214.
(30) Peterson, G. I.; Schwartz, J. J.; Zhang, D.; Weiss, B. M.; Ganter, M. A.; Storti, D. W.; Boydston, A. J. Production of Materials with Spatially-Controlled Cross-link Density via Vat Photopolymerization. *ACS Appl. Mater. Interfaces* **2016**, *8*, 29037-29043.
(31) Brown, T. E.; Malavé, V.; Higgins, C. I.; Kotula, A. P.; Caplins, B. W.; Garboczi, E. J.; Killgore, J. P. Voxel-Scale Conversion Mapping Informs Intrinsic Resolution in Stereolithographic Additive Manufacturing. *ACS Appl. Polym. Mater.* **2020**.
(32) ASTM International. *ISO/ASTM52921-13(2019) Standard Terminology for Additive Manufacturing-Coordinate Systems and Test Methodologies*. ASTM International: West Conshohocken, PA, 2019.

(33) Yu, K.; Shi, Q.; Li, H.; Jabour, J.; Yang, H.; Dunn, M. L.; Wang, T.; Qi, H. J. Interfacial Welding of Dynamic Covalent Network Polymers. *J. Mech. Phys. Solids* **2016**, *94*, 1-17.
(34) Canadell, J.; Goossens, H.; Klumperman, B. Self-Healing Materials Based on Disulfide Links. *Macromolecules* **2011**, *44*, 2536-2541.
(35) Shi, Q.; Yu, K.; Dunn, M. L.; Wang, T.; Qi, H. J. Solvent Assisted Pressure-Free Surface Welding and Reprocessing of Malleable Epoxy Polymers. *Macromolecules* **2016**, *49*, 5527-5537.

TOC IMAGE